International Journal of Pharmaceutics 421 (2011) 82–93

Contents lists available at SciVerse ScienceDirect

International Journal of Pharmaceutics

journal homepage: www.elsevier.com/locate/ijpharm

Impact of short range hydrophobic interactions and long range electrostatic forces on the aggregation kinetics of a monoclonal antibody and a dual-variable domain immunoglobulin at low and high concentrations

Vineet Kumar[a,*,1], Nitin Dixit[b,1], Liqiang (Lisa) Zhou[c], Wolfgang Fraunhofer[d]

[a] Pharmaceutics, Global Pharmaceutical Sciences, 100 Research Drive, Abbott Bioresearch Center, Worcester, MA 01605, USA
[b] Department of Pharmaceutical Sciences, School of Pharmacy, University of Connecticut, Storrs, CT, USA
[c] Protein Analytics, Global Pharmaceutical Operations, Abbott Bioresearch Center, Worcester, MA, USA
[d] Pharmaceutics, Drug Product Development, Global Pharmaceutical Sciences, Abbott Park, IL, USA

ARTICLE INFO

Article history:
Received 27 May 2011
Received in revised form 17 August 2011
Accepted 19 September 2011
Available online 21 September 2011

Keywords:
Aggregation
High concentration protein formulations
Hydrophobic interactions
Low-ionic formulations
Second virial coefficient

ABSTRACT

The purpose of this work was to determine the nature of long and short-range forces governing protein aggregation kinetics at low and high concentrations for a monoclonal antibody (IgG1) and a dual-variable-domain immunoglobulin (DVD-Ig™). Protein–protein interactions (PPI) were studied under dilute conditions by utilizing the methods of static (B_{22}) and dynamic light scattering (k_D). PPI in solutions containing minimal ionic strengths were characterized to get detailed insights into the impact of ionic strength on aggregation. Microcalorimetry and susceptibility to denature at air–liquid interface were used to assess the tertiary structure and quiescent stability studies were conducted to study aggregation characteristics. Results for IgG1 showed that electrostatic interactions governed protein aggregation kinetics both under dilute and concentrated conditions (i.e., 5 mg/mL and 150 mg/mL). For DVD-Ig™ molecules, on the other hand, although electrostatic interactions governed protein aggregation under dilute conditions, hydrophobic forces clearly determined the kinetics at high concentrations. This manuscript shows for the first time that short-range hydrophobic interactions can outweigh electrostatic forces and play an important role in determining protein aggregation at high concentrations. Additionally, results show that although higher-order virial coefficients become significant under low ionic strength conditions, removal of added charges may be used to enhance the aggregation stability of dilute protein formulations.

1. Introduction

Monoclonal antibodies (mAbs), dual-variable-domain Igs (DVD-Ig™s) and novel Fc fusion proteins are the fastest growing class of new therapeutic molecules. MAbs are increasingly being utilized for the treatment of immunological and oncological disorders and constitute a major portion (>60%) of the total protein drugs currently in clinical and preclinical testing (Morhet, 2008; Wu et al., 2007; Samaranayake et al., 2009). Many diseases that are being targeted by these relatively low potency proteins are chronic and require frequent dosing, and providing at home-outpatient administration option to patients by the sub-cutaneous or intra-muscular route is the desired way of delivery to increase patient compliance. The volume limitation (<1.5 mL) presented by these delivery routes, however, necessitates that the antibody and Ig-like therapeutics be typically formulated at high concentrations (>100 mg/mL) (Liu et al., 2005).

Development of stable, easy to use, high concentration liquid protein formulations poses several challenges including those associated with the issues of aggregation, viscosity and solubility (Shire et al., 2004). The large volume fraction (>0.1) occupied by the solutes present in these formulations can lead to significant deviations from the ideal solution conditions typically present in dilute situations (Hall and Minton, 2003; Rivas and Minton, 2004). Non-ideality leads to enhanced protein–protein attractive interactions which increase the propensity of the molecules to aggregate. It has been realized that aggregation and concentration usually have a non-linear relationship, and that aggregation could increase tremendously with an increase in the concentration of the protein (Saluja and Kalonia, 2008). It has been reported that aggregates could be less efficacious and/or may have immunogenic potential, and it is prevalently accepted that aggregation is one of the most serious challenges that pharmaceutical scientists face during the development, processing and manufacturing of these high concentration protein formulations (Shire et al., 2004).

* Corresponding author. Tel.: +1 860 634 0688; fax: +1 508 754 6742.
E-mail addresses: Vineet.Kumar@Abbott.com, vkuconn@yahoo.com (V. Kumar).
[1] Both authors contributed equally.

0378-5173/$ – see front matter © 2011 Elsevier B.V. All rights reserved.
doi:10.1016/j.ijpharm.2011.09.017

Aggregation in most cases is believed to be a two-step process that occurs when protein molecules partially unfold and associate to form reversible/irreversible higher-order complexes (Brems et al., 1988; Grillo et al., 2001; Lumry and Eyring, 1954; Manning et al., 1989). The second step of the two-step aggregation process is dependent on protein–protein attractive interactions (attractive PPI) or the colloidal stability (as determined by the DLVO theory) of the concerned protein molecules (Chi et al., 2003; Kendrick et al., 1998). In dilute solutions, the colloidal stability (i.e., PPI) is mainly determined by the long-range electrostatic interaction forces (Saluja et al., 2007a,b). The short intermolecular separation distances (≈2 nm at 120 mg/mL concentration of a typical antibody with a hydrodynamic diameter of ≈11 nm) at high concentrations may however result in significantly enhanced contributions of some of the several short-range forces (Chari et al., 2009; Saluja and Kalonia, 2008). Hydrophobic interaction forces have been observed to increase exponentially at separation distances of less than 10 nm (Isrealachvili and Pshley, 1982). Chari et al. (2009) have also shown good correlation between the calculated dipole moments and the viscoelastic behavior for a concentrated model IgG2 mAb solutions lending support to the hypothesis that short-range forces may determine protein properties at higher concentrations. However, no experimental data exist that show that one or more of these short-range forces can dominate long-range charge–charge forces and hence be the critical determinants of the aggregation kinetics at high concentrations. The question of whether or not low concentration accelerated stability data are suitable to predict high concentration real-time protein stability has engaged pharmaceutical preformulation and formulation scientists for a long time, and typically differences in experimental set-up and sample conditions intrinsic to such studies have been cited to explain differences between accelerated stability or thermo-biophysical characterization and real-time studies. Parameters that may differ include protein concentration (e.g., 1 vs. 150 mg/mL), sample stress temperature (e.g., 5 °C vs. 40 °C or temperatures exceeding the temperature onset of unfolding), and time (minutes vs. years). In this paper, we try to provide additional insight to this fundamental realm of protein stability by providing first experimental evidence that the impact of short range hydrophobic interactions and long range electrostatic forces can crucially depend on the protein concentrations used for relevant studies.

In this paper, we have characterized interaction behavior of two molecules (1) a monoclonal antibody (mAb, 147 kDa) and (2) a dual-variable-domain immunoglobulin (DVD-Ig™, 200 kDa) (Wu et al., 2007), under various dilute conditions, by utilizing the universally accepted methods for characterizing PPI, i.e., static (B_{22}) and dynamic light scattering (k_D) (Demoruelle et al., 2002; Curtis et al., 1998; Eberstein et al., 1994; George et al., 1997; Neal et al., 1999; Rosenbaum and Zukoski, 1996; Saluja et al., 2007b; Valente et al., 2005; Zimm, 1946). Microcalorimetry and susceptibility to denature at air–liquid interface have been used to characterize the folded nature of the molecules, and real-time and accelerated stability studies have been conducted to study their aggregation characteristics. We show that for some molecules such as mAb, electrostatic interactions govern protein aggregation kinetics both under dilute and concentrated solution conditions. For such molecules, B_{22} and/or k_D data obtained under dilute conditions may be utilized to predict the relative aggregation behavior under various concentrated formulation conditions (Le Brun et al., 2009). It should be realized that it is for the first time that PPI as measured at low protein concentrations have been shown to correlate with the observed aggregation kinetics at high concentrations. Previously, a research group had studied aggregation of a model IgG2 molecule at 50 mg/mL and authors acknowledged that the low storage modulus at 50 mg/mL conditions indicates that short-range forces were not significant at these concentrations (Saluja et al., 2007a).

Moreover, we show that for certain other proteins such as DVD-Ig™, although electrostatic interactions can determine protein aggregation kinetics under dilute conditions; hydrophobic interactions can become the main governing interaction force at high concentrations. If hydrophobic interactions outbalance electrostatic interactions, then naturally B_{22} and/or k_D are very poor predictors of the aggregation behavior. To the best of our knowledge, we provide first evidence that short-range forces such as hydrophobic interactions can play a governing role in driving aggregation at high concentrations.

To gain additional insight into the impact of ionic strength on PPI, we also characterized PPI in solutions containing minimal added salts (i.e., ionic strengths of less than 1 mM). Although under these conditions several higher order virial coefficients become significant (i.e., B_{222}, B_{2222}, etc.) and determine the net protein interactions, results show that for dilute protein formulations (≈1 mg/mL), significantly enhanced aggregation stability may be obtained by formulating in low-ionic solutions.

In essence the manuscript provides answers to some very relevant questions that have yet remained uninvestigated:

(1) Is there a correlation between dilute solution thermodynamic parameter B_{22}, and low concentration aggregation propensity? Can we correlate the low concentration aggregation data to aggregation data at high concentrations and hence be able to anticipate high concentration aggregation profile using B_{22} measured under dilute conditions?
(2) Are the forces governing aggregation kinetics similar at low and high concentrations?
(3) What advantage does low ionic and/or self buffering solutions provide in terms of the shelf stability of low and/or high concentration solutions (IS < 5 mM)?

2. Materials and methods

A humanized monoclonal antibody was constructed from human IgG1 framework (mAb). This antibody was cloned and expressed in a Chinese Hamster Ovary (CHO) cell line and purified at Abbott Bioresearch Center (Worcester, MA) using a three step purification process involving protein-A and ion exchange chromatography resins. A dual specific tetravalent humanized IgG like molecule, i.e., dual-variable-domain antibody (DVD-Ig™) was engineered from two antibodies (Wu et al., 2007). The two parent antibodies used to engineer the DVD-Ig™ molecule were targeting two different mediators known to contribute to the overall disease pathogenesis by distinct mechanisms. The DVD-Ig™ molecule was also cloned and expressed in a Chinese Hamster Ovary (CHO) cell line and purified at Abbott Bioresearch Center (Worcester, MA). All buffer reagents and excipients were of highest purity grade and were obtained from VWR International. High quality autoclaved and double distilled water was used for the preparation of all sample and buffer solutions. Acetate obtained from Sigma (Fair Lawn, NJ) was used for pH 4.5, Histidine obtained from JT Baker (Phillipsburg, NJ) for pH 6 and Tris obtained from JT Baker (Phillipsburg, NJ) for pH 8. Ionic strength was maintained with NaCl from JT Baker (Phillipsburg, NJ). In solutions with ionic strengths of 1 mM, appropriate buffer concentration was used such as to obtain the desired ionic strength. Solutions with total ionic strengths of 20 mM and 100 mM had 10 mM buffer strength.

2.1. Dynamic and static light scattering

Dynamic and static light scattering studies were conducted at different pH and ionic strength conditions at 25 ± 0.1 °C using a Malvern Zetasizer Nano (Worcestershire, UK). For DLS and SLS

measurements, buffers and protein solutions were filtered through 0.1 μm Millipore Milex syringe filters. The protein solutions were centrifuged at ambient temperatures on a mini centrifuge at 5600 × *g* for 10 min immediately before measurements. Low-volume glass cuvettes (Hellma, Germany) requiring 45 μL of sample volume were used for measurements. The Malvern Zetasizer Nano utilizes a 632.8 Helium Neon laser and analyzes the scattered light at an angle of 173°, reducing dust interference during back scattering measurements and reducing background noise signals. Instrument parameters were set to acquire dynamic and static light scattering data during one experiment. For a particular concentration of the protein, the instrument was first used to measure the total static light scattered by the solution and then used to obtain the dynamic light scattering data. Both measurements were made in automatic mode. Simultaneous measurement of SLS and DLS provided an advantage over measurements at different time points. The simultaneous measurements implied that the dynamic light scattering data could be utilized to acquire information about the contribution of the dust towards the total measured static light scattering intensity. The contribution of dust (if any) was hence subtracted and only the net light scattered by the protein molecules in the solution was used to obtain the second virial coefficient (B_{22}) values.

The scattered light intensity is related to the molecular weight and B_{22} by the following equation (Curtis et al., 1998; Neal et al., 1999; Tanford, 1961; Zimm, 1946).

$$\frac{Kc}{R_\theta} = \frac{1}{M_w} + 2B_{22}c + B_{222}c^2 + \cdots$$

where K is optical constant and is given by

$$K = \frac{[2\pi n(dn/dc)]^2}{N_A\lambda^4}$$

R_θ is the excess Rayleigh ratio, i.e., a measure of light scattered by the solute, n is the solvent refractive index, dn/dc is the refractive index increment of the solute, N_A is the Avogadro's number, and λ is the wavelength of the incident light. Since for most dilute solutions, higher order virial coefficients have negligible values, the following equation (Debye) is used to obtain the second virial coefficients.

$$\frac{Kc}{R_\theta} = \frac{1}{M_w} + 2B_{22}c$$

Values of B_{22} reflects the magnitude of the first deviations from ideality, its sign reflects the nature of this deviation. A positive value corresponds to net repulsive interactions between the solute molecules wherein the osmotic pressure increases above that for an ideal solution whereas a negative value corresponds to net attractive interactions between the solute molecules with a consequent decrease in solution osmotic pressure below that for an ideal solution. R_θ was obtained utilizing the scattering intensities (toluene was used as the reference standard).

$$R(\theta) = \frac{I_A n(O)^2}{I_T n(T)^2} R(T)$$

In the above equation, I_A is the residual scattering intensity of the analyte (obtained by subtracting solvent scattering intensity from the scattering intensity of the analyte solution), I_T is the toluene scattering intensity, $n(O)$ and $n(T)$ are the refractive indices of the protein and toluene solution respectively, and $R(T)$ is the Rayleigh ratio of toluene. The dn/dc values were measured for various solutions of given antibody and DVD-Ig™ molecule and an average value hence obtained, i.e., 0.187 was used for all B_{22} calculations. The dn/dc value of 0.187 is consistent with what has been reported for IgG's in literature.

Diffusion coefficients as obtained using dynamic light scattering were also used to quantitate the nature of PPI in solution. The mutual diffusion coefficient as obtained is related to the self-diffusion coefficient by the following equation (Andries et al., 1983; Narayanan and Liu, 2003; Veldkamp and Votano, 1976)

$$D_m = D_s(1 + k_D c)$$

In which k_D (slope) is a measure of the inter-particle interaction and is represented by (Zhang and Liu, 2003):

$$k_D = 2B_{22}M_w - \zeta_1 - 2\upsilon_{sp}$$

where ζ_1 is the coefficient of the linear term in the virial expansion of the frictional coefficient as a function of solute concentration and υ_{sp} is the partial specific volume of the solute. The last two terms represent the hydrodynamic contribution. B_{22} on the other hand is a thermodynamic parameter representing the impact of chemical potential on the process of diffusion.

Stokes Einstein's equation was used to calculate the hydrodynamic diameter (d_H)

$$D_m = \frac{kT}{3\pi\eta d_H}$$

wherein k is the Boltzmann constant, T is the absolute temperature and η is the solution viscosity.

2.2. Differential scanning calorimetry

DSC was used to characterize the thermodynamic stability of the proteins under various solution conditions. An automated cap DSC instrument from Microcal (Northampton, MA) was used. The thermal scans were obtained from 25 °C to 95 °C at a scan rate of 60 °C/h. A prescan equilibration thermostat of 10 min was applied before each scan. A corresponding buffer scan was taken immediately following the sample scan. Protein concentration of 1 mg/mL was used to obtain the scans and all scans were run in duplicate. The difference in T_m was less than 0.8 °C between repeat scans. Following buffer subtraction and normalization, the scans were fitted to a non two state cursor initiated model to obtain the thermodynamic parameters and the T_m values.

2.3. Susceptibility to denature at air–liquid interface

1 mg/mL protein solutions in 6R glass vials (5 mL fill) were shaken on an IKA H-260 shaker (Wilmington, NC) at 150 rpm for extended periods of time at ambient temperature. At specified time points, the optical density of the solutions undergoing shaking was determined using a Varian CaryWin UV spectrometer. Following measurements, the solutions were transferred back to the 6R vials to ensure sample volumes were held constant throughout the shaking studies.

2.4. Accelerated and real-time stability studies

For mAb, the concentrations of the samples kept on stability were 5 mg/mL and 150 mg/mL, respectively. For DVD-Ig™ molecules, the concentrations used were 5 mg/mL and 100 mg/mL, respectively. For the preparation of samples, the protein solutions at 5 mg/mL were buffer exchanged using Pierce 10,000 molecular weight cut off dialyzing cassettes (Rockford, IL). Amicon, Millipore (Cork, Ireland) ultracentrifugation tubes were then used to concentrate the samples to slightly greater than the required values. Finally, the high concentration samples were diluted with the appropriate buffers to the target concentrations, subjected to 0.45 μm filtration and filled in 0.5 mL sterile tubes under a laminar hood.

Analysis of the stability samples was conducted using HPLC/UV following separation on a TSK G3000 SWX_L gel filtration column. 100 mM sodium phosphate buffer at pH 7 containing 200 mM sodium sulfate was used for elution. A flow rate of 0.3 mL/min was utilized for all samples and quantitation of the fractionated specimen was performed using conventional UV detection at 214 nm (and 280 nm).

2.5. SDS PAGE

Accelerated stability samples of DVD-Ig™ were fractionated by SEC to collect the aggregate and monomer fractions. These fractions were analyzed by SDS-PAGE under both reducing and non-reducing conditions. The protein samples were mixed with SDS sample buffer (in the presence of DTT in the reducing condition) and incubated at 70 °C for 15 min. Samples were loaded to 8–16% Tris-glycine gel (8 μg load per lane) and electrophoresis was run at 125 kV. The gel was stained by colloidal blue staining.

2.6. Dynamic scanning fluorescence

DSF was used to characterize the thermodynamic stability of low and high concentration mAb and DVD-Ig™ solutions. An automated high throughput instrument from Avacta (York, UK), Optim-1000 was used for the study. 9 μL MCAs (cuvettes) were used and the study was done in duplicate. For preparation of stock samples, 3 μL Sypro orange (Invitrogen, Cambridge, MA) was added to 27 μL sample solution such as to obtain a final 1× concentration of the dye. The dye is available as 5000× commercial product and is a proprietary molecule. The thermal scans were obtained from 30 °C to 90 °C at a scan rate of 60 °C/h.

3. Results and discussion

Because of the increase in the molecular mass and the structural complexity, it was anticipated that the biophysical stability of this specific DVD-Ig™ molecule may not necessarily be similar to that generally observed for mAbs. In some of the preliminary studies it was observed that the DVD-Ig™ molecule indeed had a higher propensity to aggregate and denature at interfaces and hence it became necessary to mechanistically investigate the nature of these PPI and to study its impact on aggregation kinetics.

3.1. Protein–protein interactions

Static light scattering (SLS) and dynamic light scattering (DLS) have comprehensively been used to characterize the nature of PPI in dilute protein solutions and the data have been shown to correlate well to the aggregation propensity of the solutions containing low to medium protein concentrations (5–50 mg/mL) (Saluja et al., 2007a,b). The SLS and DLS data obtained by these authors have also been shown to align well with the viscoelastic behavior of high concentration protein solutions (>100 mg/mL). Light scattering studies were hence undertaken to characterize the nature of PPI. Fig. 1 shows the Debye plots for the DVD-Ig™ molecule at pH 6.0 under various ionic strength conditions. Debye equation was fitted to the light scattering data for solutions containing ionic strengths of 1, 20 and 100 mM. The positive values of B_{22} (slope) indicate that PPI are repulsive in nature. It becomes obvious that

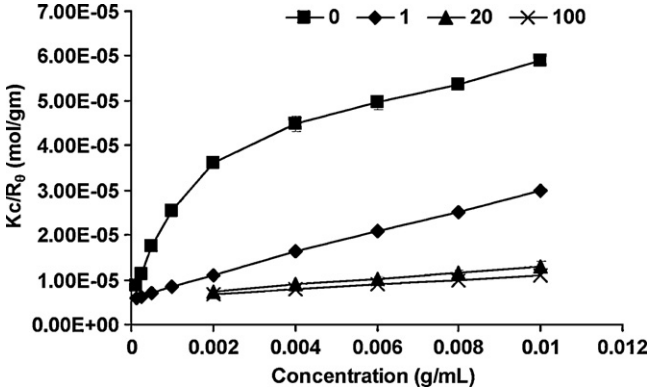

Fig. 1. Debye plots for DVD-Ig™ solutions at pH 6.0 under different ionic strength conditions. The second virial coefficients and the molecular weights obtained from the slope and intercept, respectively have been summarized in Tables 1 and 2. The measurements were conducted at 25 ± 0.1 °C in duplicates for each solution. The error bars are deviations from average. Lines are guide to eyes and not the result of the linear fitting of the data.

the repulsions increased with the decrease in the ionic strength of the solution. Considering the fact that the iso-electric point of DVD-Ig™ molecule is pH 9.0, it is not unreasonable that an increase in ionic strength by the addition of NaCl at a pH value away from the pI results in a decrease in the repulsive interactions between the positively charged DVD-Ig™ molecules. Especially noticeable is the profile of the Debye plot for the solution of the protein in absence of any ions (i.e., at ≈0 mM ionic strength). It has been known for a long time that proteins in solution have self-buffering capacity that can outweigh the buffering capacity of buffer excipients typically used in protein formulations (Bukatsch, 1980; Hardcastle, 1981). The growing interest in the area of low-ionic formulations led us to pursue the characterization of PPI in protein–water binary solutions. In the absence of any added charges, the Debye plot shows significant deviations from linearity indicating that higher order virial coefficients become important under these conditions. Extreme non-ideality of such solutions thus necessitated that the data be fitted to the more complex equation (Tanford, 1961):

$$\frac{Kc}{R_\theta} = \frac{1}{M_w} + 2B_{22}c + 3B_{222}c^2 + 4B_{2222}c^3 + 5B_{22222}c^4$$

The results of the fit are summarized in Table 1 ($R^2 > 0.9999$). The significance of the extremely high positive B_{22} values is worth mentioning. For most dilute solutions, B_{22}, a parameter that quantifies the first deviations from ideality, is given by the slope of the linear Debye plot obtained when Kc/R_θ is graphed against the concentration of the protein. However, for the solution of the protein in water, this dilute condition regime is valid only until about 1 mg/mL protein concentration (Fig. 1). The value of the B_{22} that would be obtained using this early part of the curve should be similar to the one that has been obtained above (i.e., using data from the entire curve). Since PPI could determine the propensity of the protein molecules to aggregate (Saluja et al., 2007a), high repulsive interactions present in low-ionic solutions show that such conditions could be used to enhance the aggregation stability of proteins, especially those that are formulated at low concentrations (<1 mg/mL).

Table 1
Values of the virial coefficients as obtained following fitting the equation to data. The errors are deviations from average.

Sample	pH	$B_{22} \times 10^4$ (mol mL/g^2)	$B_{222} \times 10^2$ (mol mL^2/g^3)	$B_{2222} \times 10^1$ (mol mL^3/g^4)	$B_{22222} \times 10^{-2}$ (mol mL^4/g^5)	$M_w \times 10^{-3}$ (Da)
DVD-Ig™	6.0	136 ± 5.77	−273.8 ± 16.6	3376.1 ± 339	−221 ± 35.8	189 ± 14
mAb	6.0	202 ± 7.64	−502 ± 51.3	7630 ± 1310	−588 ± 132	138 ± 8

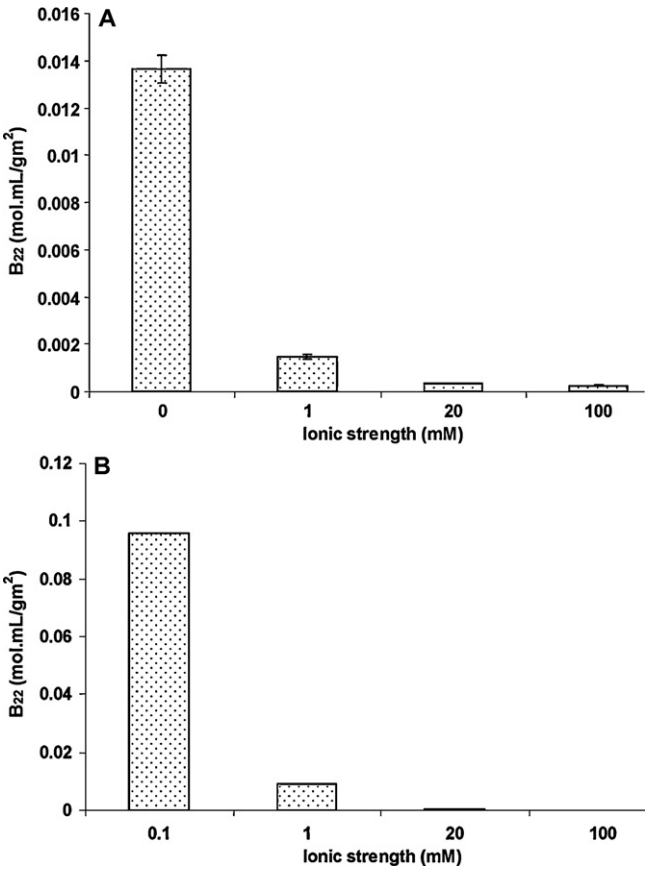

Fig. 2. Impact of ionic strength on the experimental (A) and theoretical (B) B_{22} values for the DVD-Ig^{TM} molecule at pH 6.0. The experimental results as plotted are taken from Tables 1 and 2. The theoretical result has been calculated using the relationship given by Winzor.

Winzor et al. (2007) have previously defined the following theoretical equation to describe the pairwise excluded volume interactions between two spherical molecules in solution:

$$B_{22} = \frac{16\pi N_A R^3}{3} + \frac{Z^2(1+2\kappa R)}{4I(1+2\kappa R)^2}$$

where N_A is Avogadro's number, R is the radius of the molecule, Z is the net charge spread uniformly over the surface, and I is the ionic strength. The inverse screening length κ is given by $3.27 \times 10^7 \times (I)^{1/2}\ \mathrm{cm}^{-1}$. The above equation shows that B_{22} and ionic strength have an inverse correlation and that B_{22} values should increase (and induce repulsive PPI) with a decrease in the ionic strength of the solution. Furthermore, the equation shows that such an increase should achieve tremendous proportions when extreme low-ionic strength conditions are reached. The equation was hence used to calculate the B_{22} values for the DVD-Ig^{TM} molecule at pH 6.0 (where the theoretical charge has been calculated to be 40). Although, qualitatively, data aligns extremely well with theoretical prediction (Fig. 2), the experimental B_{22} values are smaller than that of theoretical calculations. The reason for such discrepancy is unclear. Antibodies have been observed to have an affinity for the negatively charged ions (Bull et al., 1978) and hence it is possible that the effective charge on the DVD-Ig^{TM} molecule is reduced because of potential salt/ion binding. This would imply that the theoretical B_{22} values obtained using the net charge of 40 are overestimations of the true values. Electrophoretic measurements of pI values however indicated little ion binding. Another possible explanation of the variation in the true and the experimental B_{22} values could be the fact that the

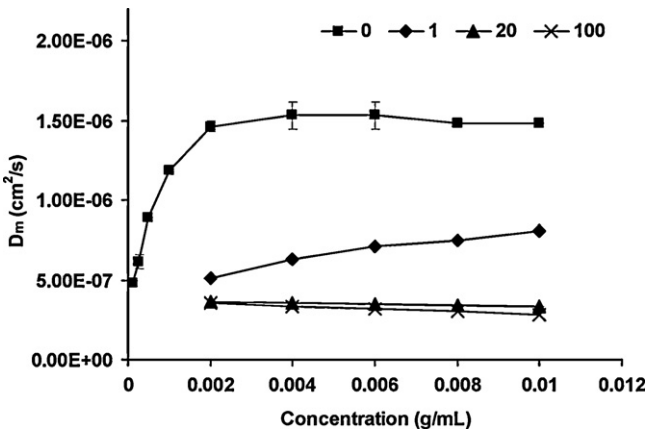

Fig. 3. Mutual diffusion coefficients for the DVD-Ig^{TM} molecule as a function of concentration and solution ionic strength at pH 6.0 and 25 ± 0.1 °C measured using DLS. The measurements were conducted in duplicate. The error bars are deviations from average. Lines are guide to eyes and not the result of the linear fitting of the data.

true ionic strengths of the 0 mM solutions cannot be an absolute 0. Despite the use of extensive dialysis techniques, excluded volume and Donnan effects actively restrict the minimum ionic strength conditions that could be achieved. The minimum ionic strength that is achieved also depends on the ratio of the volumes of the buffers in the permeate and the retentate chambers. However, ionic strength measurements of the solutions used in this work and ionic strength calculations showed that the ionic strength of the protein–water binary solutions used for the work presented in this manuscript did not exceed 0.05 mM. The data clearly raises a question mark in regard to the validity of the theoretical equation used for the comparison. For one, the equation certainly does not incorporate the effect of much of the hydrophobic interactions.

Fig. 3 shows the effect of solution ionic strength and protein concentration on the measured mutual diffusion coefficient values (D_m) for the DVD-Ig^{TM} molecule at pH 6.0. As mentioned earlier, the slope of the curves (k_D) obtained following the linear regression analysis of the data is a measure of inter-particle interactions (Saluja et al., 2007b):

$$k_D = 2B_{22}M_w - \zeta_1 - 2\upsilon_{sp}$$

Since diffusivity is dependent on the apparent size of the molecule, it should be clear that a higher positive slope indicates greater repulsive PPI. From Fig. 3 it can be seen that with increasing solution ionic strength PPI become more attractive and less repulsive. The overall behavior of the DVD-Ig^{TM} molecule as characterized from DLS data is thus consistent with SLS measurements. Although SLS and the DLS data match perfectly, the slopes of the curves at ionic strength conditions of 20 and 100 mM seem to have different signs (Figs. 1 and 3). This observation can be explained based on the nature of interactions contributing to the SLS and the DLS of a macromolecular solution. It has been explained earlier that the last two terms in the above equation represent the hydrodynamic interactions and the first term involving B_{22} represents the thermodynamic contribution. Saluja et al. (2007b) have shown that in the concentration range of up to 10 mg/mL, DLS measurements are significantly affected by the hydrodynamic interactions of the solute molecules. The negative slopes at ionic strengths of 20 and100 mM suggest that under these solution conditions the contribution of the hydrodynamic term exceeds the contribution of the thermodynamic term.

For DVD-Ig^{TM} molecules, B_{22} and k_D measurements were also performed under a variety of other formulation conditions and similar measurements were conducted for mAb as well. The results of these measurements are summarized in Tables 1 and 2. Several

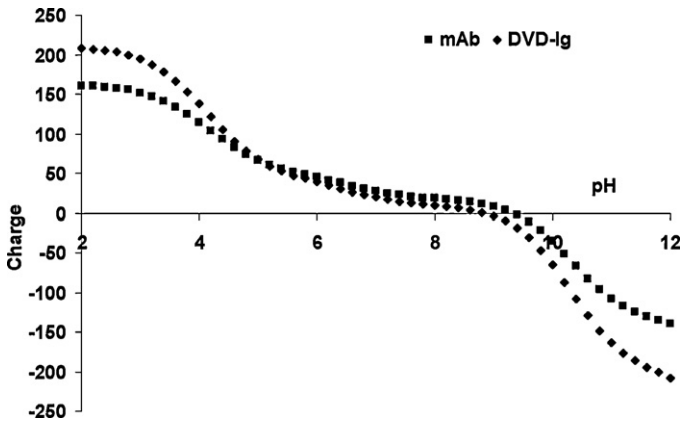

Fig. 4. Calculated theoretical net charge on the mAb and the DVD-Ig™ molecule.

important conclusions can be drawn from these results. At any particular ionic strength condition, for both mAb and DVD-Ig™ molecules the B_{22} values increased with a decrease in the solution pH. Since both proteins have pI values of around 9.0, these results are not surprising. Fig. 4 shows the calculated theoretical net charge on both the mAb and the DVD-Ig™ molecule at different pH conditions. Lowering the pH increases the net positive charge of the molecules leading to the observed increase in the repulsive interactions. These results show that under dilute conditions (<10 mg/mL), electrostatic interactions contribute significantly towards determining the overall PPI. Self-diffusion coefficients (D_s) that were obtained following the linear regression analysis of the mutual diffusion coefficient data are also listed in Table 2. The average self-diffusion coefficient values were used to calculate the hydrodynamic diameters of the two proteins using Stokes–Einstein equation. The diffusion coefficients corresponded to the hydrodynamic diameter of 10.8 nm and 13.1 nm for mAb and DVD-Ig™ molecules respectively. The value calculated for mAb is in good alignment for the value expected for a typical antibody molecule measured under such conditions (Bermudez and Forciniti, 2004). Given the fact that the molar mass of the DVD-Ig™ molecule is 200 kDa and exceeds typical mAb values by 50 K, a hydrodynamic diameter of 13.10 nm for DVD-Ig™ molecule seems reasonable. An additional observation is that for both proteins the experimental molar masses as obtained from the Debye plots seem to fall short of the true molecular mass values. The reason for such an observation has recently been pointed out by some authors (Yadav et al., 2011). Although on the lower side, considering the variations usually obtained in the light scattering and the refractive index data (±10%) reported by other authors (Bajaj et al., 2004), we believe that the numbers as obtained are reasonable. Additionally, since the data is more for a qualitative purpose rather than for a quantitative utility, the conclusions are justified.

3.2. Accelerated and real time shelf stability

In order to characterize the impact of formulation conditions on the susceptibility of the molecules to form soluble aggregates (little insoluble aggregates were observed), and to provide additional insight into the nature of PPI that are critical in determining aggregation kinetics, protein samples were kept under identical conditions at various temperatures for various times and aggregation was monitored over time. Just prior to starting accelerated and real-time stability, samples were pulled and monomer, aggregate and fragment levels of the pulled samples was determined using SEC (T_0 samples). The net change in the level of monomer, aggregate and/or fragment at any later time point was hence determined simply by subtraction and addition, respectively.

Fig. 5A and B shows the impact of ionic strength on the percentage aggregates formed in samples of mAb at pH 6.0 following storage at 40 °C for 3 months. Solutions at ≈0 mM ionic strength exhibited the lowest amount of aggregates at both 5 mg/mL and 150 mg/mL concentrations. The aggregate level increased with an increase of the ionic strength of the solution. Moreover, the aggregation propensity was found to be almost similar for solutions having ionic strengths of 20 and 100 mM. It should be realized that even a slight increase of the ionic strength of the protein solution, i.e., within a 0–20 mM range, was found to significantly enhance the aggregation propensity. This is demonstrated by the % difference in the level of aggregates between the samples formulated at ≈0 and 1 mM ionic strength conditions for solutions containing protein concentration of 5 mg/mL. The leveling off in the amount of aggregates being formed at or above the ionic strength of 20 mM indicates that very low ionic strength levels are sufficient to completely diminish the repulsive PPI present under these conditions. Although the impact of ionic strength on the aggregation propensity is quite similar for solutions having protein concentrations of 5 and 150 mg/mL, one subtle difference is noticeable. The change in aggregate levels between solution with ≈0 and 1 mM ionic strength is much lower for high protein concentration solutions (150 mg/mL) than the difference detected in low protein concentration solutions (5 mg/mL mAb). The profile of the Kc/R_θ

Table 2
Parameters calculated for the mAb and the DVD-Ig™ using static and dynamic light scattering measurements at 25 ± 0.1 °C. The errors are deviations from average.

Sample	pH	Ionic strength (mM)	$D_s \times 10^7$ (cm²/s)[a]	k_D (mL/g)[b]	$B_{22} \times 10^4$ (mol mL/g²)[c]	$M_w \times 10^{-3}$ (Da)[d]
DVD-Ig	4.5	1	3.42 ± 0.04	434.90 ± 15.31	26.09 ± 0.82	195 ± 1
DVD-Ig	4.5	20	3.66 ± 0.004	5.96 ± 0.32	5.08 ± 0.03	168 ± 2.89
DVD-Ig	4.5	100	3.60 ± 0.03	−13.33 ± 0.88	3.09 ± 0.07	160 ± 3.38
DVD-Ig	6	1	3.41 ± 0.06	379.28 ± 51.34	14.71 ± 1.09	183 ± 0.57
DVD-Ig	6	20	3.75 ± 0.02	−11.04 ± 1.37	3.37 ± 0.06	163 ± 2.35
DVD-Ig	6	100	3.70 ± .002	−23.05 ± 0.02	2.51 ± 0.19	170 ± 3.40
DVD-Ig	8	1	3.81 ± 0.01	−4.74 ± 0.06	3.50 ± 0.05	155 ± 0.78
DVD-Ig	8	20	3.73 ± 0.02	−27.31 ± 0.29	2.14 ± 0.03	162 ± 5.08
DVD-Ig	8	100	3.66 ± 0.03	−25.33 ± 0.90	2.34 ± 0.07	164 ± 4.59
mAb	4.5	1	4.16 ± 0.03	463.93 ± 0.01	37.21 ± 0.96	128 ± 7.35
mAb	4.5	20	4.43 ± 0.02	5.77 ± 0.74	5.65 ± 0.03	123 ± 3.52
mAb	4.5	100	4.41 ± 0.02	−12.25 ± 0.41	3.56 ± 0.12	112 ± 3.85
mAb	6	1	4.23 ± 0.01	267.47 ± 5.19	16.05 ± 0.13	132 ± 7.35
mAb	6	20	4.35 ± 0.003	−18.21 ± 0.24	3.16 ± 0.03	138 ± 2.04
mAb	6	100	4.41 ± 0.01	−28.38 ± 0.30	2.03 ± 0.04	123 ± 1.73

[a] From intercept (e.g., Fig. 3).
[b] Slope (e.g., Fig. 3).
[c] Slope(e.g., Fig. 1).
[d] Intercept (e.g., Fig. 1).

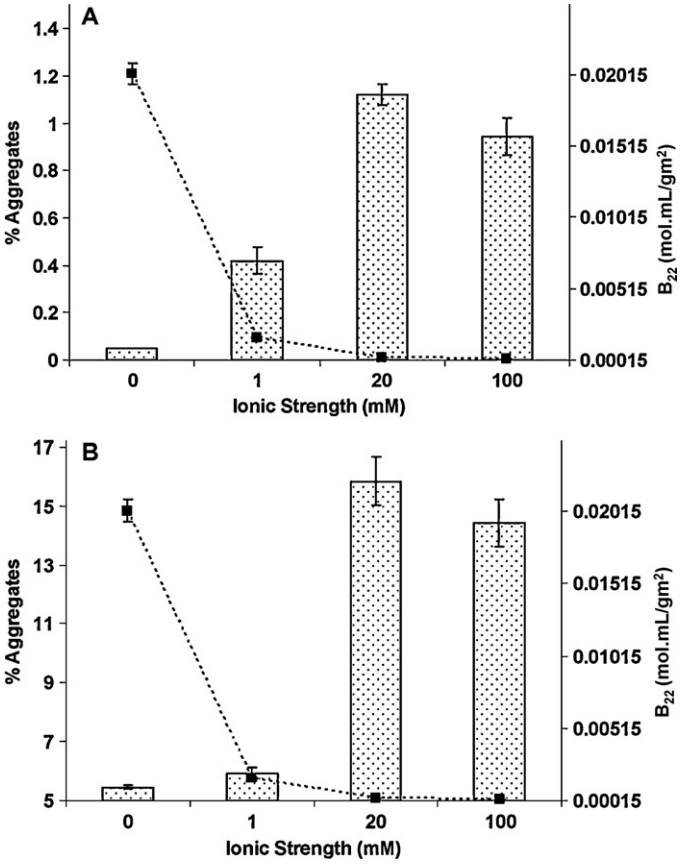

Fig. 5. Percent aggregates formed after storing the mAb solution for 3 months at 40 °C at different ionic strength conditions. (A) 5 mg/mL solutions and (B) 150 mg/mL solutions. Samples were kept in duplicate. The measurements were conducted in duplicate. The error bars are deviations from average.

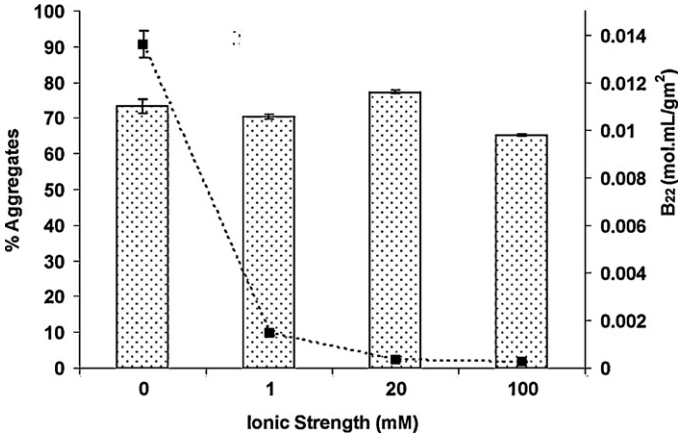

Fig. 6. Percent aggregates formed after storing the DVD-Ig™ solution at 40 °C at different ionic strength conditions. 100 mg/mL solutions following 21 days storage. Samples were kept in duplicate. The measurements were conducted in duplicate. The error bars are deviations from average.

vs. concentration plots can be used to explain this behavior (please note that for mAb, the profiles looked exactly similar to that of DVD-Ig™). The non-linearity of the slope and/or the decrease of the slope with an increase in the concentration of the protein (evident from Fig. 1) for solutions with ≈0 mM ionic strengths predicts that the difference in PPI between ≈0 and 1 mM ionic strength conditions should be significantly lower for the solution that has 150 mg/mL protein concentration than for the solution that have lower protein concentrations, e.g., 1 mg/mL, 5 mg/mL or 20 mg/mL. Studies are ongoing in our lab to verify whether real-time data reflects this prediction. The figures also show the values of the second virial coefficients obtained under the different ionic strength conditions used for accelerated and real-time stability studies. Qualitatively, the behavior of PPI indicated by B_{22} values obtained under dilute conditions correlate very well with the behavior of aggregation observed for 5 mg/mL concentration conditions as well as for 150 mg/mL concentration. These results show that minimum aggregation was observed at conditions where B_{22} values were most positive. B_{22} values at 20 and 100 mM ionic strength were little different from each other when compared to the values of B_{22} obtained at 0 and 1 mM ionic strength conditions. Evidently, the kinetics of aggregation at 20 and 100 mM ionic strengths is also quite similar. It is well accepted that among the various interactions, electrostatic forces play the predominant role in determining PPI in dilute solutions. In the present case, the impact of ionic strength on B_{22} clearly suggests the same conclusion. It should be clear to the reader that even though the aggregation may be driven by hydrophobic forces, the kinetics at both low and high concentrations is governed by charge and hence long-range electrostatic interactions. It is clear that for some proteins such as mAb, B_{22} can be used to qualitatively predict the relative aggregation behavior under various formulation conditions for both low and high concentration formulations. To the best of our knowledge, it is for the first time that B_{22} data obtained under dilute conditions have been correlated to the aggregation behavior obtained at concentrations of up to 150 mg/mL, considering parameters such as storage temperature, ionic strength, and formulation pH.

The results for the impact of solution ionic strength on the level of aggregates formed in samples of DVD-Ig™ when stored at 40 °C under dilute conditions (5 mg/mL) at pH 6.0 for 3 months were found to be qualitatively very similar to that observed for mAb (data not shown). The aggregation propensity increased with an increase in the ionic strength of the solution. The rate of aggregation was similar at 20 and 100 mM ionic strength conditions, indicating (as for mAb) that very low levels of ionic strength can effectively reduce the repulsive PPI present at pH values away from the pI. Similar trends were also observed for solutions at pH 4.5 confirming that the ionic strength dependency of the aggregation propensity of DVD-Ig™ is similar to that observed for mAb. Both B_{22}, and storage stability studies thus show that electrostatic interactions are the primary forces governing PPI and hence aggregation kinetics within the DVD-Ig™ molecules under dilute conditions. These results strengthen the conclusion that for both molecules, mAb and DVD-Ig™, conformational stability of the native state is not the rate determining step in the process of aggregation at least at low concentrations (ionic strengths within 0–100 mM range did not affect the melting transitions as determined by DSC, data not shown). The effect of ionic strength on the rate of aggregation at pH 6.0 was also measured at 100 mg/mL concentrations for DVD-Ig™ (Fig. 6). The aggregation propensity did not show any trend and was indifferent to the ionic strength conditions. Clearly, the impact of ionic strength disappears under these high concentration conditions. PPI and hence protein aggregation within the DVD-Ig™ molecules at high concentrations thus seem to be determined by forces that are not affected by the ionic strength of the solution.

The differential trends observed at low and high concentration for the DVD-Ig™ could be explained in two ways. It is possible that at high concentrations the rate limiting step in the aggregation of the DVD-Ig™ molecules shifts from second (colloidal stability) to the first (conformational stability). This however is only possible if the thermodynamic stability of the DVD-Ig™ solutions is significantly affected by the concentration of the protein. Limitations in the techniques available for such high concentration thermal stability assessments put forward a tough task ahead of us. Limited

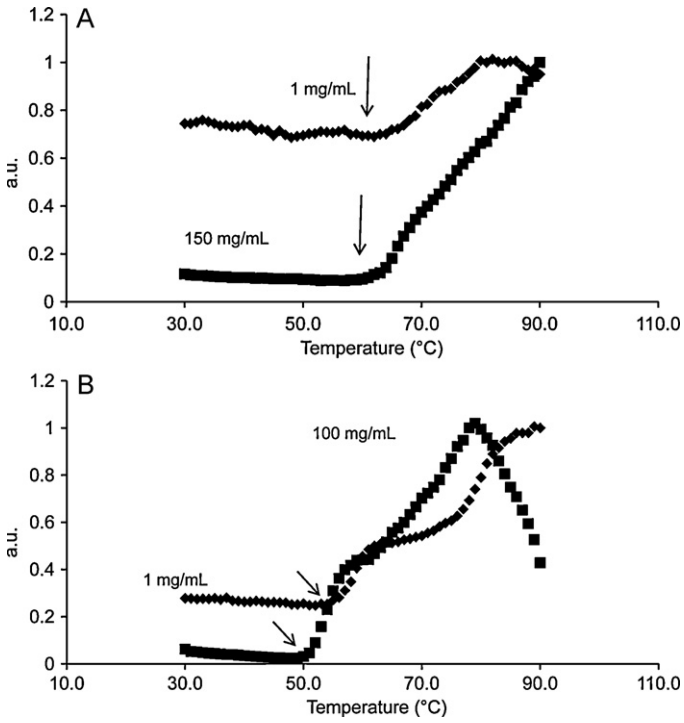

Fig. 7. Impact of protein concentration on the thermal stability of mAb and DVD-Ig™ molecules as assessed by extrinsic florescence using sypro orange dye at pH 6.0 (IS = 20 mM). (A) mAb and (B) DVD-Ig™.

analysis was however performed using extrinsic dye fluorescence. Fig. 7 shows the results for the thermal unfolding of the low and high concentration formulations of mAb and DVD-Ig™. Onset of unfolding was observed to shift from 63 to 61 °C for mAb and from 54 to 51 °C for the DVD-Ig™. Slight changes in the observed thermodynamic stability thus are unable to explain the observed differential trends of the two molecules at different concentrations.

The other possible and more realistic explanation comes to mind if one takes a look at the different possible interaction forces that may exist at low and/or high concentrations. In solutions of charged proteins, the potential between two interacting molecules can be expressed by the following equation (Larson, 1999; McMillan and Mayer, 1945):

$$W_{22}(r) = W_{hs}(r) + W_{charge}(r) + W_{disp}(r) + W_{osm}(r) + W_{ass}(r) + W_{dip}(r)$$

where W_{hs} is the hard sphere potential, W_{charge} is the energetic potential comprising of charge–charge interactions, W_{disp} is the van der Waals dispersion potential, W_{osm} is the added potential due to the osmotic effect of the salt, W_{ass} is the square-well potential and accounts for the hydrophobic interactions, W_{dip} represents the interactions arising from the permanent and induced dipole moment of the molecule and comprises of charge–dipole, dipole–dipole, charge–induced dipole, induced dipole–induced dipole, and charge fluctuation contributions. In certain models of protein self association, some of the short-range interactions such as hydrophobic interactions, specific ionic interactions and van der Waals interactions are grouped under an associative potential that can assume a square well form when a specific site on one protein is within a certain distance of a different site on another protein molecule (Chari et al., 2009). Under dilute conditions, W_{charge} plays the predominant role unless the molecules have a tendency to self-associate when the contribution from the last two terms may become significant as well (Elcock and McCammon, 2001). In concentrated solutions, any one or more of the other

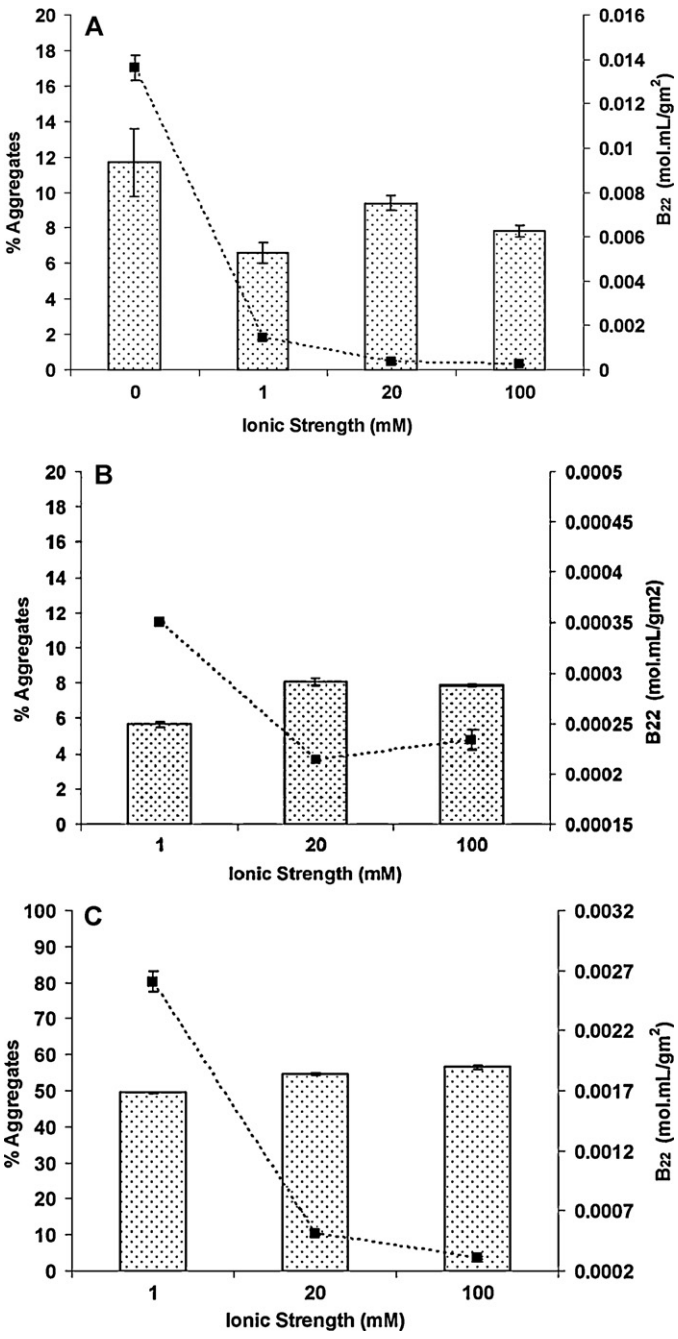

Fig. 8. Percent aggregates formed after storing the DVD-Ig™ solution for 3 months at 5 °C at different ionic strength conditions. (A) 100 mg/mL solutions at pH 6.0, (B) 100 mg/mL solutions at pH 8.0 and (C) 100 mg/mL solutions at pH 4.5. Samples were kept in duplicate. The measurements were conducted in duplicate. The error bars are deviations from average.

short-range forces may contribute significantly and hence determine protein properties in such solutions (short-range forces fall off rapidly with distance due to a higher order inverse dependence on center–center distance). It is important to consider that only charge–charge and excluded volume hard sphere interactions are repulsive in nature. The contribution of most of the attractive forces independent of the range of the force is anticipated to decrease with an increase in the ionic strength of the solution (Lockhart and Kim, 1993). Charge–charge and van der Waals interactions (including dipole interactions) have been shown to vary significantly on the addition of the salt (Lockhart and Kim, 1993; Saluja et al., 2007a). The only short-range attractive forces

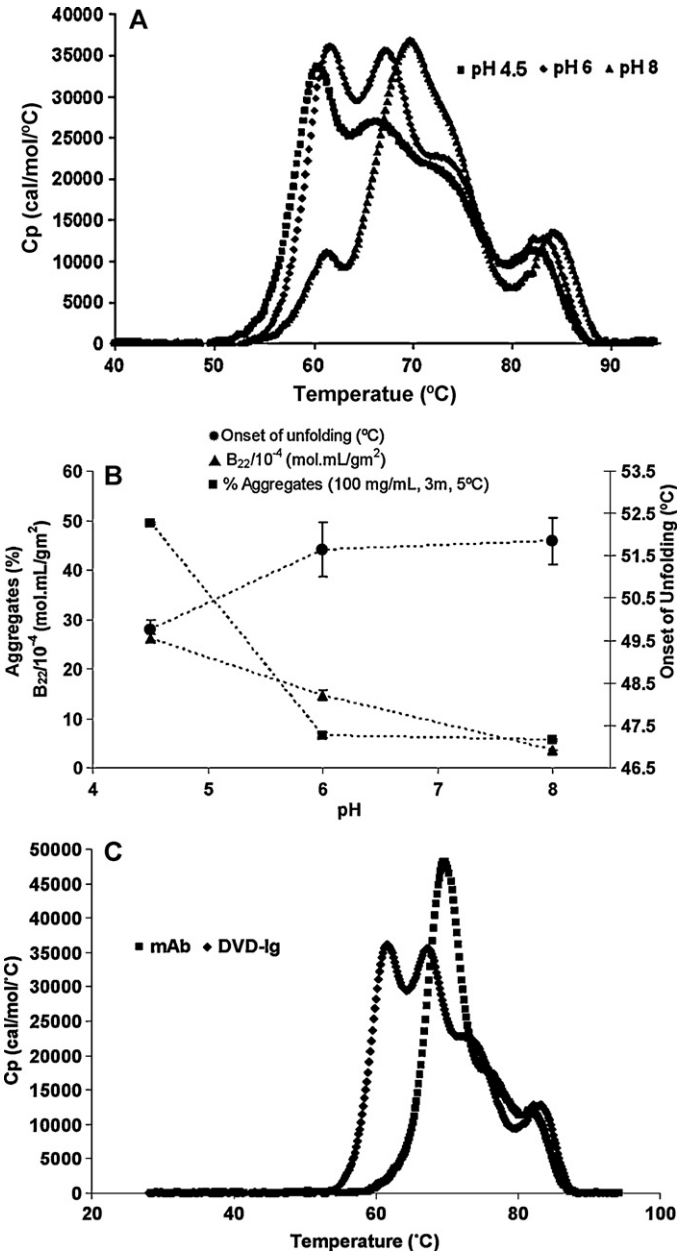

Fig. 9. Thermodynamic stability of DVD-Ig™ and the mAb and the relationship between physical stability and thermal stability. (A) Impact of pH on the thermograms of DVD-Ig™ measured at 1 mg/mL concentrations. (B) Correlation between the impact of pH on the onset of unfolding of the first transition and the % aggregation following three months storage at 1 mM conditions. (C) Thermograms for the DVD-Ig™ and mAb at pH 6.0 (IS 1 mM) measured at 1 mg/mL concentration conditions. The DSC measurements were done in duplicate and the difference between the midpoint of transitions in the repeat scans was less than 0.2°.

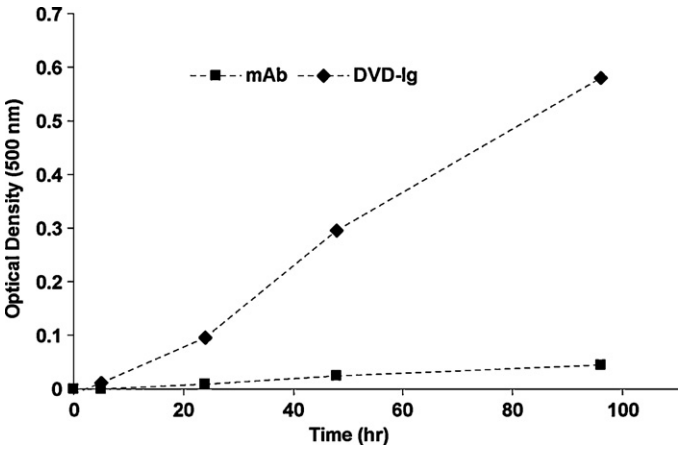

Fig. 10. Effect of shaking at 150 rpm on an IKA shaker in 5 mL typical freeze drying vials on the optical density (OD_{500}) of the samples of DVD-Ig™ and the mAb at pH 6.0, 1 mg/mL concentration conditions. The measurements were conducted in duplicate. The error was less than 5%.

unaffected by the ionic strength of the solution especially in the range 0–20 mM, are hydrophobic interactions (Jando et al., 1986; Mancera, 1998). It is important to notice that high salt concentrations (1–2 M) may however enhance hydrophobic attractions by preferential exclusion mechanism (Jando et al., 1986; Mancera, 1998). Hydrophobic forces have been observed to be the major determinant of protein aggregation in some high concentration solutions (Chennamsetty et al., 2009). Above results for DVD-Ig™ molecules clearly indicate that hydrophobic forces outweigh electrostatic interactions and hence govern aggregation kinetics of the DVD-Ig™ molecules at high concentrations.

Stability studies for the DVD-Ig™ molecule were also conducted at 5 °C under various ionic strength and pH conditions such as to mechanistically investigate the nature of interactions under the real time stability conditions and to confirm that hydrophobic interactions are indeed the forces that govern PPI at high concentrations. Fig. 8A–C shows the impact of ionic strength on the aggregation propensity of the DVD-Ig™ molecule at 100 mg/mL at pH 6.0, pH 8.0 and pH 4.5 respectively. For pH 6.0 (i.e., at a pH away from the pI of the molecule), it is anticipated that addition of salt should decrease the repulsive PPI and increase the rate of aggregation. Results however indicate that the aggregation propensity does not show any trend and is not as significantly affected by the addition of salt (Fig. 8A). The results obtained at 5 °C are similar to data obtained at 40 °C. Overall, the aggregation propensity was also observed to be almost identical at pH 6.0 and pH 8.0 (compare to data of 1, 20 and 100 mM ionic strength conditions in Fig. 8A and B). Since PPI at pH 8.0 are least repulsive due to formulation pH close to the PI and the calculated net charge being virtually zero for both mAb and DVD-Ig™ (refer to Fig. 4), it was expected that DVD-Ig™ would have higher propensity to aggregate at pH 8. The absence of any significant effect of ionic strength and/or pH (pH 6 and pH 8) on the rate of formation of aggregates at 5 °C further supports the conclusion that short-range hydrophobic interactions are indeed the major contributors to PPI within the DVD-Ig™ molecules at 100 mg/mL concentrations. The enhancement of the hydrophobic effect at concentrated conditions thus seems to reduce the colloidal stability of the molecule and hence reduce the energy barrier of the rate limiting step in the process of DVD-Ig™ molecule aggregation.

3.3. Thermal stability

In order to further gain insight into the mechanism of aggregation, DSC experiments were conducted under various formulation conditions to characterize the thermodynamic stability of the DVD-Ig™ molecules. Thermodynamic stability is an indicator of the conformational stability of the molecule and of the buried nature of the hydrophobic residues within the protein core, these studies should provide a better understanding of the underlying cause of the enhanced propensity of the DVD-Ig™ molecule to aggregate at high concentrations (Ionescu et al., 2008). Fig. 9A shows the DSC thermograms of the DVD-Ig™ molecule at pH 4.5, 6.0 and 8.0 at an ionic strength of 1 mM (it was observed that ionic strengths within 0–0.1 M range did not affect the melting transitions). Combining conclusions from DSC data with data from

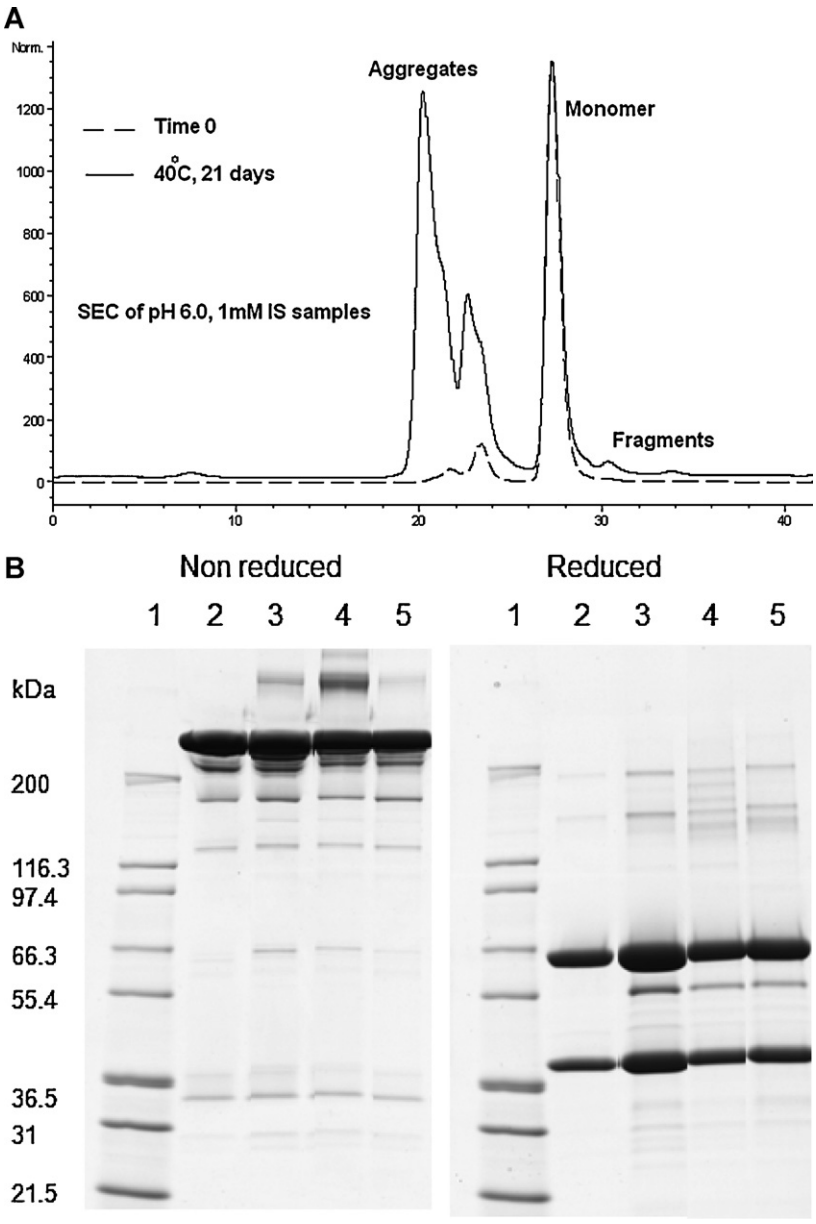

Fig. 11. Nature of aggregates of DVD-Ig^{TM} as obtained following collection of the different fractions using SEC. (A) Example chromatograms and (B) reduced and non reduced gels of the aggregates and monomer fractions, Lines: (1) protein standard; (2) time 0; (3) 40 °C, 21 day sample; (4) 40 °C, 21 day sample, aggregate sample and (5) 40 °C, 21 day sample, monomer sample.

accelerated and real-time stability studies helps provide further insight into the main forces governing aggregation: Four unfolding transitions were observed for DVD-Ig^{TM} molecules compared to three generally observed for mAbs. The three transitions in mAb arise because of the rather independent unfolding of the CH_2, CH_3 and the Fab domains of the molecule (Ionescu et al., 2008). DVD-Ig^{TM} molecules contain one additional variable domain that is connected to the first variable domain by a 6–12 amino acid linker (Chengbin et al., 2007), and the additional unfolding transition observed in DSC studies can be associated with the unfolding of this extra domain in the DVD-Ig^{TM} molecule. Transition temperatures and the temperatures of the onset of unfolding were observed to be lowest at pH 4.5. Lowest thermodynamic stability at pH 4.5 condition may indicate that hydrophobic residues are more prone to exposure at this pH and/or are exposed to a greater extent at this pH (certainly a possibility that the hydrophobic sites are more exposed because of the greater intra-molecular repulsive interactions). Less compact dynamic structures should translate into greater intermolecular hydrophobic interactions and hence into higher propensity of the molecules to aggregate in solution during real-time studies and especially during accelerated stability studies. Fig. 9B shows the correlation between the onset of unfolding temperatures, the B_{22} values and the % aggregates formed following three months storage stability at high concentrations (5 °C) for the DVD-Ig^{TM} molecule. For high concentration solutions, incubation at 40 °C resulted in complete degradation within a time period of 40 days, and it became imperative to utilize the 5 °C data (it has been demonstrated previously that the mechanism of aggregation is similar at the two different temperature conditions). Clearly, not B_{22} but structural stability appears to correlate well with the propensity of the molecules to aggregate at high concentrations (B_{22} correlates well at low concentrations as observed previously). Fig. 9C compares the DSC thermograms for a typical antibody such as mAb and the DVD-Ig^{TM} molecule at pH 6.0

conditions. The first unfolding transition of the DVD-Ig™ molecule is detected at much lower temperature when compared to the first transition of a typical mAb. Lower conformational stability for the DVD-Ig™ molecule as compared to that of the mAb also suggests that the DVD-Ig™ molecule may have a greater propensity to aggregate via mechanisms governed by hydrophobic interactions.

3.4. Stability against shaking stress

Fig. 10 compares the optical densities at 500 nm for the DVD-Ig™ and the mAb molecules following shaking for different time periods. The proneness to aggregate at the air–liquid interface as indicated by the values of OD_{500} is much higher for the DVD-Ig™ molecule. Typical values of OD_{500} for antibodies in general are similar to that observed here for mAb. Susceptibility to aggregate at air–liquid interface is dependent on the PPI as determined by the electrostatic charge on the molecules and/or the structural stability of the molecules (Maa and Hsu, 2000; Treuheit et al., 2009). Given the fact that B_{22} values at pH 6.0 were quite similar for mAb and DVD-Ig™ molecules long-range electrostatic interactions do not seem to be the reason for the observed difference in the proneness to aggregate when exposed to interfaces. The higher propensity for the DVD-Ig™ molecule to form insoluble aggregates at the air–liquid interface suggests that the molecules have greater probability to interact via hydrophobic interactions. Greater propensity to unfold and expose hydrophobic residues thus explains the observed phenomenon.

3.5. Nature of aggregates

The nature of the aggregates formed in the stability studies was investigated by DSC and reduced and non reduced gels following collection of the aggregate and monomer fractions using SEC. Fig. 11 shows and the gel profiles of the various species. Results show that the aggregates are predominantly (>80%) non-covalent in nature. DSC results also showed that the aggregates unfolded 1–2 °C earlier than the monomer but otherwise were not significantly different in the profile (the thermal scan for the solution used in DSC was stopped at around 55 °C and rerun in SEC which showed that the material was not different from the material we started with). Shaking studies also indicate that the DVD has significant propensity to interfacial aggregation which may suggests that the protein is prone to partial unfolding. However some authors do not completely agree to this partial unfolding theory such as Kiese et al., who have observed that nonnative aggregates mainly form on exposure to heat stress while shaking induced mechanical stress results in soluble native aggregates (Kiese et al., 2008, 2009). Of course it is hard to quantify partial unfolding and hence the dilemma. Detailed characterization of the aggregates is underway and the work will form part of future publications.

4. Conclusions

In this work we determined the nature of long and short-range forces governing protein–protein interactions (PPI) and hence protein aggregation kinetics at low (5 mg/mL) and high concentrations (up to 150 mg/mL) for a monoclonal antibody (IgG1) and a dual-variable-domain antibody (DVD-Ig™). It was shown that electrostatic interactions governed DVD-Ig™ aggregation under dilute conditions at low protein concentrations, while short-range hydrophobic forces determined aggregation kinetics at high DVD-Ig™ concentrations. We hope that these findings and the conclusions provided help scientists explain real-time and accelerated stability data and help better assess a scenario where forces governing aggregation at low protein concentration can be of different nature and origin than aggregation relevant forces at high protein concentrations. We also have characterized the nature of PPI under dilute conditions using static and dynamic light scattering over a broad ionic strength range, even in the absence of any added charges where sample solutions did not contain buffer or other ionic excipients. Although several higher order virial coefficients (i.e., B_{222}, B_{2222}, etc.) become significant and determine the net protein interactions under low-ionic strength conditions, results clearly suggest that protein aggregation can be dramatically reduced (least for IgG's) by formulating in salt free solutions. We expect that the impact of ionic strength on physico-chemical characteristics of high concentration antibody formulations and ways to beneficially exploit these findings in the realm of protein stabilization and protein drug product development will become an important focus of academic and industrial research.

References

Andries, C., Guedens, W., Clauwaert, J., Geerts, H., 1983. Photon and fluorescence correlation spectroscopy and light scattering of eye-lens proteins at moderate concentrations. Biophys. J. 43, 345–354.

Bajaj, H., Sharma, V.K., Kalonia, D.S., 2004. Determinations of the second virial coefficients of proteins using a dual-detector cell for simultaneous measurements of scattered light intensity and concentration. Biophys. J. 87, 4048–4055.

Bermudez, O., Forciniti, D., 2004. Aggregation and denaturation of antibodies: a capillary electrophoresis, dynamic light scattering, and aqueous two phase partitioning study. J. Chromatogr. B 807, 17–24.

Brems, D.N., Plaisted, S.M., Havel, H.A., Tomich, C.C., 1988. Stabilization of an associated folding intermediate of bovine growth hormone by site-directed mutagenesis. Proc. Natl. Acad. Sci. USA 85, 3367–3371.

Bukatsch, F., 1980. Simple experiment for the detection of the amphoteric character of albumin solutions (buffer effect). Praxis der Naturwissenschaften, Chemie 29, 348.

Bull, T., Norne, J.E., Reimarsson, P., Lindman, B., 1978. Nuclear magnetic resonance studies of chloride binding to proteins. J. Am. Chem. Soc. 100, 4643–4647.

Chari, R., Jerath, K., Badkar, A., Kalonia, D.S., 2009. Long- and short-range electrostatic interactions affect the rheology of highly concentrated antibody solutions. Pharm. Res. 26, 2607–2618.

Chengbin Wu, Ying, H., Grinnel, C., Bryant, S., Miller, R., Clabbers, A., Bose, S., McCarthy, D., Zhu, R-R., Santora, L., Davis-Taber, R., Kunes, Y., Fung, E., Schwartz, A., Sakorafas, P., Gu, J., Tarcsa, E., Murtaza, A., Ghayur, T., 2007. Simultaneous targeting of multiple disease mediators by a dual-variable-domain immunoglobulin. Nat. Biotechnol. 25, 1290–1297.

Chennamsetty, N., Helk, B., Voynov, V., Kayser, V., Trout, B.L., 2009. Aggregation prone motifs in human IgG. J. Mol. Biol. 391, 404–413.

Chi, E.Y., Krishnan, S., Kendrick, B.S., Chang, B.S., Carpenter, J.F., Randolph, T.W., 2003. Roles of conformational stability and colloidal stability in the aggregation of recombinant human granulocyte colony-stimulating factor. Protein Sci. 12, 903–913.

Curtis, R.A., Prausnitz, J.M., Blanch, H.W., 1998. Protein–protein and protein–salt interactions in aqueous protein solutions containing concentrated electrolytes. Biotechnol. Bioeng. 57, 11–21.

Demoruelle, K., Guo, B., Kao, S., Heather, M.M., Dragan, B.N., Steven, C.H., Wilson, W.W., 2002. Correlation between the osmotic second virial coefficient and solubility for equine serum albumin and ovalbumin. Acta Crystallogr. D: Biol. Crystallogr. 58, 1544–1548.

Eberstein, W., Georgalis, Y., Saenger, W., 1994. Molecular interactions in crystallizing lysozyme solutions studied by photon correlation spectroscopy. J. Cryst. Growth 143, 71–78.

Elcock, A.H., McCammon, J.A., 2001. Calculation of weak protein–protein interactions: the pH dependence of the second virial coefficient. Biophys. J. 80, 613–625.

George, A., Chiang, Y., Guo, B., Arabshahi, A., Cai, Z., Wilson, w.w., 1997. Second virial coefficient as predictor in protein crystal growth. Methods Enzymol. 276, 100–110.

Grillo, A.O., Edwards, K.L.T., Kashi, R.S., Shipley, K.M., Hu, L., Besman, M.J., Middaugh, C.R., 2001. Conformational origin of the aggregation of recombinant human factor VIII. Biochemistry 40, 586–595.

Hall, D., Minton, A.P., 2003. Macromolecular crowding: qualitative and semi-quantitative successes, quantitative challenges. Biochim. Biophys. Acta 1649, 127–139.

Hardcastle, J.E., 1981. Buffer action of proteins. J. Chem. Ed. 58, 726.

Ionescu, R.M., Vlasak, J., Price, C., Kirchmeier, M., 2008. Contribution of the variable domains to the stability of humanized IgG1 monoclonal antibodies. J. Pharm. Sci. 97, 1414–1426.

Isrealachvili, J., Pshley, R., 1982. The hydrophobic interaction is long-range, decaying exponentially with distance. Nature 300, 341–342.

Jando, M., Yano, Y., Nishida, H., Nishida, T., 1986. Effect of salt on inter and intra molecular hydrophobic interactions in macromolecules. J. Sol. Chem. 15, 839–850.

Kendrick, B.S., Cleland, J.L., Lam, X.M., Nguyen, T., Randolph, T.W., Manning, M.C., Carpenter, J.F., 1998. Aggregation of recombinant human interferon gamma: kinetics and structural transitions. J. Pharm. Sci. 87, 1069–1076.
Kiese, S., Pappenberger, A., Friess, W., Mahler, H.C., 2008. Shaken, not stirred: mechanical stress testing of an IgG1 antibody. J. Pharm. Sci. 97, 4347–4366.
Kiese, S., Pappenberger, A., Friess, W., Mahler, H.C., 2009. Equilibrium studies of protein aggregates and homogeneous nucleation in protein formulation. J. Pharm. Sci. 99, 632–644.
Larson, R.G., 1999. The Structure and Rheology of Complex Fluids. Oxford University Press, New York.
Le Brun, V., Friess, W., Schultz-Fademrecht, Torsten, Muehlau, S., Garidel, P., 2009. Lysozyme–lysozyme self-interactions as assessed by the osmotic second virial coefficient: impact for physical protein stabilization. Biotechnol. J. 4, 1305–1319.
Liu, J., Nguyen, M.D., Andya, J.D., Shire, S.J., 2005. Reversible self association increases the viscosity of a concentrated monoclonal antibody in aqueous solution. J. Pharm. Sci. 94, 1928–1940.
Lockhart, D.J., Kim, P.S., 1993. Electrostatic screening of charge and dipole interactions with the helix backbone. Science 260, 198–202.
Lumry, R., Eyring, H., 1954. Conformation changes of proteins. J. Phys. Chem. 58, 10–120.
Maa, Y.F., Hsu, C.C., 2000. Protein denaturation by combined effect of shear and air–liquid interface. Biotechnol. Bioeng. 54, 503–512.
Mancera, R.L., 1998. Does salt increase the magnitude of the hydrophobic effect? A computer simulation study. Chem. Phys. Lett. 296, 459–465.
Manning, M.C., Patel, K., Borchardt, R.T., 1989. Stability of protein pharmaceuticals. Pharm. Res. 6, 903–918.
McMillan, J.W.G., Mayer, J.E., 1945. The statistical thermodynamics of multicomponent systems. J. Chem. Phys. 13, 276–305.
Morhet, J., 2008. Improving therapeutic antibodies. Drug Deliv. Technol. 8, 76–79.
Narayanan, J., Liu, X.Y., 2003. Protein interactions in undersaturated and supersaturated solutions: a study using light and x-ray scattering. Biophys. J. 84, 523–532.
Neal, B.L., Asthagiri, D., Velev, O.D., Lenhoff, A.M., Kaler, E.W., 1999. Why is the osmotic second virial coefficient related to protein crystallization? J. Cryst. Growth 196, 377–387.
Rivas, G., Minton, A.P., 2004. Non ideal tracer sedimentation equilibrium: a powerful tool for the characterization of macromolecular interactions in crowded solutions. J. Mol. Recognit. 17, 362–367.
Rosenbaum, D.F., Zukoski, C.F., 1996. Protein interaction and crystallization. J. Cryst. Growth 169, 752–758.
Saluja, A., Badkar, A., Zeng, D.L., Kalonia, D.S., 2007a. Ultrasonic rheology of a monoclonal antibody (IgG2) solution: implications for physical stability of proteins in high concentration formulations. J. Pharm. Sci. 96, 3181–3195.
Saluja, A., Badkar, A., Zeng, D.L., Nema, S., Kalonia, D.S., 2007b. Ultrasonic storage modulus as a novel parameter for analyzing protein–protein interactions in high protein concentration solutions: correlation with static and dynamic light scattering measurements. Biophys. J. 92, 234–244.
Saluja, A., Kalonia, D.S., 2008. Nature and consequences of protein–protein interactions in high protein concentration solutions. Int. J. Pharm. 358, 1–15.
Samaranayake, H., Wirth, T., Schenkwein, D., Raty, J.K., Yla-Herttuala, S., 2009. Challenges in monoclonal antibody-based therapies. Ann. Med. 41, 322–331.
Shire, S.J., Shahrokh, Z., Liu, J., 2004. Challenges in the development of high protein concentration formulations. J. Pharm. Sci. 93, 1390–1402.
Tanford, C., 1961. Physical Chemistry of Macromolecules. John Wiley and Sons, New Jersey.
Treuheit, M.J., Kosky, A.A., Brems, D.N., 2009. Inverse relationship of protein concentration and aggregation. Pharm. Res. 19, 511–516.
Valente, J.J., Payne, R.W., Manning, M.C., Wilson, W.W., Henry, C.S., 2005. Colloidal behavior of proteins: effects of the second virial coefficient on solubility, crystallization and aggregation of proteins in aqueous solution. Curr. Pharm. Biotechnol. 6, 427–436.
Veldkamp, W.B., Votano, J.R., 1976. Effects of intermolecular interaction on protein diffusion in solution. J. Phys. Chem. 80, 2794–2801.
Winzor, D.J., Deszczynski, M., Harding, S.E., Wills, P.R., 2007. Nonequivalence of second virial coefficients from sedimentation equilibrium and static light scattering studies of protein solutions. Biophys. Chem. 128, 46–55.
Wu, C., Ying, H., Grinnell, C., Bryant, S., Miller, R., Clabbers, A., Bose, S., McCarthy, D., Zhu, R.R., Santora, L., Davies-Taber, R., Kunes, Y., Fung, E., Schwartz, A., Sakorafas, P., Gu, J., Tarsca, E., Murtaza, A., Ghayur, T., 2007. Simultaneous targeting of multiple disease mediators by a dual-variable-domain immunoglobulin. Nat. Biotechnol. 25, 1290–1297.
Yadav, S., Scherer, T.M., Shire, S.J., Kalonia, D.S., 2011. Use of dynamic light scattering to determine second virial coefficient in a semidilute concentration regime. Anal. Biochem. 411, 292–296.
Zhang, J., Liu, X.Y., 2003. Effect of protein–protein interactions on protein aggregation kinetics. J. Chem. Phys. 119, 10972–10976.
Zimm, B.H., 1946. Applications of the methods of molecular distribution to solutions of large molecules. J. Chem. Phys. 14, 164–179.